



# Rainfall asymmetries of tropical cyclones prior to, during, and after making landfall in South China and Southeast United States

Weixin Xu<sup>a,\*</sup>, Haiyan Jiang<sup>b</sup>, Xianbiao Kang<sup>c</sup>

<sup>a</sup> Department of Atmospheric Sciences, Colorado State University, Fort Collins, CO, United States

<sup>b</sup> Department of Earth and Environment, Florida International University, Miami, FL, United States

<sup>c</sup> National Marine Environmental Forecasting Center, State Oceanic Administration, Beijing, China

## ARTICLE INFO

### Article history:

Received 3 October 2013

Received in revised form 12 December 2013

Accepted 26 December 2013

### Keywords:

Landfalling tropical cyclone

Tropical cyclone rainfall

TC rainfall asymmetry

Vertical wind shear effect

TC motion effect

## ABSTRACT

This study examines rainfall asymmetries of tropical cyclones (TCs) prior to, during, and after making landfall in South China and the Southeast United States from 1998 to 2011 based on TRMM rainfall products. The climatological TC rainfall asymmetries are then linked to various potential environmental factors. These factors include TC intensity and motion, vertical wind shear, topography, sea surface temperature (SST), and total precipitable water (TPW). All these factors are examined in combination, as it is in the real world. Results show that effects of the deep vertical wind shear (200–850 hPa) dominate the rainfall asymmetries producing maxima on the downshear and downshear-left sides. This wind shear effect is still dominant even during TCs making landfall, or after landfall, or interacting with mountains. The magnitude of the rainfall asymmetry increases with shear magnitude, but decreases with increasing TC intensity. Furthermore, the shear effect is less efficient for TCs over relatively cool SST and low TPW oceans when TCs produce less precipitation. On the other hand, effects of storm motion (producing rainfall maxima at front quadrants) are not evident in this study, mainly due to opposing vertical wind shear effects. However, landfalling TCs experience a significant increase in the rainfall percentage toward the right quadrants relative to the coast, likely due to surface frictional gradient between land and sea. There is no evident signature of precipitation enhancement over the windward slope of mountains (400–600 m) in SCHN and SECHN.

© 2014 Elsevier B.V. All rights reserved.

## 1. Introduction

When a tropical cyclone (TC) makes landfall, strong winds and storm surge can cause tremendous damage in coastal areas. However, the most deadly and destructive disaster produced by landfalling TCs may be inland freshwater flooding (or mudslides in mountains induced by flash flooding) caused by torrential rain (Marks and Shay, 1998; Rappaport, 2000; Chien and Kuo, 2011).

Therefore, correctly predicting the specific areas that will experience the heaviest rain is extremely important in disaster mitigation. A fundamental step is to characterize TC precipitation asymmetries and find the contributing factors (Chan et al., 2004; Lonfat et al., 2004; Chen et al., 2006). Previous studies showed that TCs both over oceans and making landfall exhibit significant rainfall (or convective activity) asymmetries (Corbosiero and Molinari, 2002; Lonfat et al., 2004; Chan et al., 2004; Chen et al., 2006; Cecil, 2007).

Early observations have generally shown that TCs over the global ocean have a precipitation maximum ahead (either front-right or front-left) of the storm center (Burpee and Black, 1989; Rodgers et al., 1994). Recently, based on satellite composites, it was found that the maximum rainfall is located

\* Corresponding author at: Department of Atmospheric Sciences, Colorado State University, 3915 W. Laporte Ave., Fort Collins, CO 80521, United States.  
E-mail address: [wXu.atmos@gmail.com](mailto:wXu.atmos@gmail.com) (W. Xu).

at the front-left quadrant for tropical storms and at the front-right for hurricanes or typhoons (Lonfat et al., 2004). Previous studies cited above have emphasized the importance of surface friction-induced low-level convergence caused by storm motion. However, more recent studies indicate that TC precipitation asymmetries are more related to the vertical wind shear (Corbosiero and Molinari, 2002; Chen et al., 2006; Ueno, 2007; Cecil, 2007). As shown in these studies, a maximum of lightning, convective activity, and rain rate occurs at the downshear and left-of-shear in the Northern Hemisphere regardless of the storm motion. The magnitude of rainfall asymmetry increases with the magnitude of the wind shear, but decreases with storm intensity. Wind shear effect overwhelms the storm motion effect on TC rainfall asymmetry, e.g., rainfall maxima is still located at the downshear or left-of-shear even storm motion plays an opposite effect.

As a TC approaches land, surface friction gradient between land and sea induces a frictional convergence to the right side of the storm motion in the Northern Hemisphere. This right side favored feature of landfalling TCs' precipitation has been shown in many observations and numerical studies (Powell, 1982; Tuleya and Kurihara, 1978). Rainfall maxima on the left side have also been found in landfalling TCs (Parrish et al., 1982; Blackwell, 2000). Rainfall maxima in left quadrants could be caused by frictional effects in recurving TCs moving northward parallel to the coastline. However, frictional convergence cannot be the only factor in determining the rainfall maximum location. Recent studies showed that rainfall distribution in landfalling TCs could be influenced by many other factors such as vertical wind shear (Chan et al., 2004; Liu et al., 2007), TPW (Jiang et al., 2008a,b; Matyas, 2010), surrounding SST (Cecil, 2007; Jiang et al., 2008a,b), interaction between TC and baroclinic systems (Atallah et al., 2007) or between TC and monsoon flows (Chien and Kuo, 2011; Lee et al., 2012), and local topographic effects (Liou et al., 2012).

The southern China and southeastern United States coasts have the greatest occurrence of TC landfalls across all TC basins (Knapp et al., 2010). Although TC rainfall asymmetries in these basins have been extensively investigated, there are less studies focusing on landfalling TCs. First of all, previous studies on the precipitation asymmetries of landfalling TCs are more case (or multiple case) based (Powell, 1982; Parrish et al., 1982; Blackwell, 2000; Chan et al., 2004; Liu et al., 2007; Liou et al., 2012). Therefore, a long-term climatology of such is very necessary. In short, important issues associated with TC rainfall asymmetries are still left to answer. For example, how does the rainfall distribution change during the life cycle (prior-to, during, and after landfall) of TCs making landfall? How do rainfall asymmetries of landfalling TCs respond to a combination of various environmental and other factors including TC motion and intensity, atmospheric dynamics and moisture, topography, and SST? Solving these issues could help to improve TC precipitation forecasts on land during landfall and could possibly be utilized as guidance by forecasters. This study is therefore motivated to investigate rainfall asymmetries of TCs that are close to landfall using different methodology and data from previous studies, and correlates rainfall asymmetries to possible influencing factors.

## 2. Data and methodology

### 2.1. Best-track, reanalysis, and precipitation datasets

The International Best Track Archive for Climate Stewardship (IBTrACS) (Knapp et al., 2010) is used in this study. The database collects and combines historical records of TC information for all TC basins from 25 agencies. As other best-track databases, the IBTrACS provides the TC center location, TC intensity, and other important characteristic parameters of TCs every 6 h. The European Centre for Medium-Range Weather Forecasts re-analysis (ERA) Interim reanalysis data (Dee and Uppala, 2009) are used to calculate the mean deep environmental vertical wind shear between 200 and 850 hPa and the TPW. SST data are taken from the daily Reynolds SST analysis (Reynolds et al., 2007).

The precipitation data used in this study are taken from Tropical Rainfall Measuring Mission (TRMM) Multi-satellite Precipitation Analysis (TMPA) 3B42 precipitation product version 7 (Huffman et al., 2007). TRMM 3B42 has 3-hourly temporal resolution and 0.25° by 0.25° spatial resolution, covering the globe from 50° S to 50° N, available from 1998 to the present. TRMM 3B42 has been frequently used for TC rainfall analysis regionally and globally (Shepherd et al., 2007; Jiang and Zipser, 2010; Prat and Nelson, in press). Based on the previous studies, TRMM 3B42 rainfall estimates perform reasonably well over southeast China and Southeast US (Huffman et al., 2007; Shen et al., 2010; Zhao and Yatagai, 2013), even for TC precipitation (Jiang et al., 2008a,b). The present TRMM 3B42 data have incorporated gauge data through PDF (probability density function) matching (Huffman et al., 2007). Shen et al. (2010) showed that the gauge-adjustment procedures applied in TRMM 3B42 remove the large-scale bias almost completely, especially for regions with dense gauge networks including southeast China. Zhao and Yatagai (2013) reported that the differences between TRMM 3B42 product and the gauge analysis of daily precipitation are within ~10% over southeast China. Jiang et al. (2008a,b) also showed that the TRMM 3B42 (RT) rainfall estimates have fairly high accuracy compared to radar and gauge data, during the landfalls of hurricanes Isidore and Lili over southeast US. For example, the overall bias of TRMM 3B42 (RT) for hurricane Lili is ~0.49 mm day<sup>-1</sup>. Based on six heavy TC rainfall events over Louisiana, USA, Habib et al. (2009) indicated that TRMM 3B42 research products have fairly low bias (<25%) and high correlation values (0.8) with relate to gauge and radar observations. The bias of TRMM 3B42 rainfall estimates might come from uncertainties of radar attenuation corrections and microwave retrievals (Huffman et al., 2007). Even though satellite-based rainfall estimates are subject to uncertainties, rain gauge measurements could also underestimate the true catch in the large surface wind environment induced by hurricanes. This study is based on composites of TCs over relatively large boxes (e.g., 10,000 km by 500 km). These averages can smooth the data field and lower the uncertainty. A major goal of this study is to examine the variability of TC rainfall asymmetry as a function of distance to the coast, i.e., prior to, during, and after TC landfalling. TRMM 3B42 data are in a good position to serve this purpose due to its high resolution, full coverage, and reasonable accuracy.

## 2.2. Selection criteria and definitions

In this study, South China and surrounding waters are divided into the southern part (SCHN; boxes 1–3 in Fig. 1a) and the eastern part (SECHN; boxes 4–6 in Fig. 1a). As will be shown later, one group of TCs tracks westward to SCHN while another group translates northwestward to SECHN after initiation over the western North Pacific. Similarly, the Southeast US and adjacent oceans are separated into the southern part (SUSA; boxes 7–9 in Fig. 1b) and the eastern part (SEUSA; boxes 10–12 in Fig. 1b). Only TC tracks that finally made landfall in these regions during 1998–2011 were selected, except in the SEUSA. Since the population of TCs directly making landfall in the SEUSA is so low (statistically not significant), non-landfalling TCs are also included (Fig. 1b). This brings twice more samples for periods of before and near landfall in SEUSA, as these periods have less than 10 TCs if only landfalling TCs are considered (Fig. 1b). As mentioned previously, the goal of this study is to investigate TC rainfall asymmetries and environment effects before, during, and after landfall. For this purpose, Chan et al. (2004) and Liu et al. (2007) examine TC rainfall asymmetry as a function of time relevant to landfall. However, this study is more interest in how rainfall asymmetries change and influenced by environments as function of distance from landfalling, since TC translation speed might vary significantly. Therefore, in each geographic region, three spatial sub-regions are defined for TCs based on their proximity to the coast as follows: (1) Off-shore – TCs still

far away from the coast (400–700 km), Pre-land – TCs close to landfall (0–300 km; or 0–400 km for SECHN to include Taiwan Island), and Aft-land – TCs after landfall (from –200 to 0 km), respectively (Fig. 1a–b). Six hourly TC snapshots are selected for each of the spatial sub-regions when TC centers fall into its area (samples shown in Table 1). TC rainfall is defined as all TRMM 3B42 precipitation occurring within a 500 km radius from the TC center (Lonfat et al., 2004; Shepherd et al., 2007; Jiang and Zipser, 2010). Though this definition might include some non-TC associated precipitation and exclude some TC rainfall, it works as an efficient proxy of TC rainfall unless very small samples are considered (Lonfat et al., 2004; Chen et al., 2006; Shepherd et al., 2007; Cecil, 2007; Jiang and Zipser, 2010; Jiang et al., 2011).

In this study, TCs were separated into three categories based upon their maximum sustained winds (MSW) value as follows: (1) tropical depressions/storms (TDs/TSs; with  $0 \text{ kt} < \text{MSW} < 64 \text{ kt}$ ); (2) category 1 to 2 hurricanes or typhoons (CAT12; with  $64 \text{ kt} < \text{MSW} < 96 \text{ kt}$ ); (3) category 3 to 5 hurricanes or typhoons (CAT35; with  $\text{MSW} > 96 \text{ kt}$ ), same as definitions by Lonfat et al. (2004) and Chen et al. (2006). TC translation vectors are calculated from two sequential 6-hourly TC centers on the track. Vertical wind shear between 200 and 850 hPa ( $V_{200} - V_{850}$ ) and TPW is derived from the ERA-Interim database. The vertical wind shear is averaged over a 200–800 km annulus around the TC center (Chen et al., 2006; Cecil, 2007), while TPW is averaged over the TC area (500 km radius).

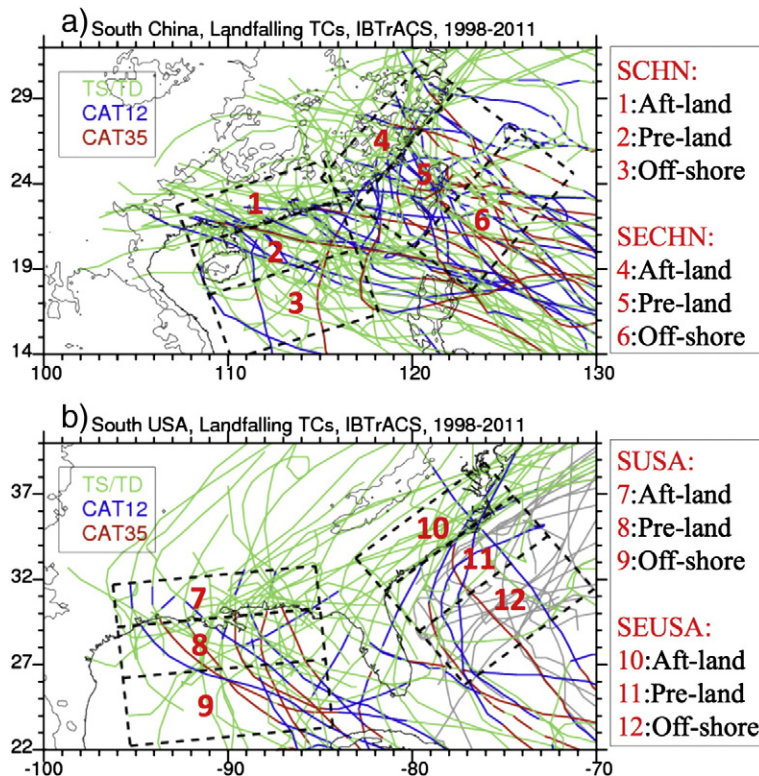


**Fig. 1.** Tracks of tropical cyclones made landfall in 1998–2011 in (a) South China and (b) Southeast US. Storm intensity is indicated by different colors. Gray tracks over Northwest Atlantic Ocean represent non-landfall TCs. Elevations above 500 m are indicated by gray contours. Dashed boxes stand for study regions in different TC stages: offshore (Off-shore), prior-to-landfall (Pre-land), and after-landfall (Aft-land).

**Table 1**

Landfalling TC population and six hourly samples in various regions shown in Fig. 1 during 1998–2011. For SEUSA, non-landfalling (number in bracket) TCs are included for study. TCs are categorized by intensity at landfall or near landfall (within 300 km from the coast).

	Tropical cyclone population				Six hourly samples		
	Total	TS/TD	CAT12	CAT35	Off-shore	Pre-land	Aft-land
SCHN	49	33	12	4	181	166	153
SECHN	42	20	14	8	142	151	100
SUSA	32	22	5	5	112	140	123
SEUSA	39	25	11	3	189	146	68
	(19)	(12)	(6)	(1)			

**3. Results**

*3.1. Landfalling TC tracks*

During the period from 1998 to 2011, a total of 91 and 52 TCs made landfall in southern China (including SCHN and SECHN) and in the southeastern US (including SUSA and SEUSA), respectively (Table 1). From this total there were 38 typhoons in the southern China and 17 hurricanes in the southeastern US by the time of landfall or near landfall. Most of the TCs that made landfall on the southern China coast originated from the warm waters of the western North Pacific ocean to the east of 130° (Fig. 1a). After developing into tropical

storms or typhoons over the western North Pacific, a group of TCs (mostly TSs) tracked down west-north-westward, crossed the Philippines, and made landfall in the SCHN region, while another group (mostly typhoons) tracked down northwestward, crossed the Taiwan Island, and made landfall in the SECHN region. It is interesting that major typhoons are more likely to move along the northern track (SECHN) than along the southern one (SCHN). In the western Atlantic basin, some TCs tracked northwestward and made landfall in the SUSA region after passing the Gulf of Mexico, while some TCs tracked northwestward and then made a northeast turn with final landfall in the SEUSA region (Fig. 1b). A few TCs crossing the SEUSA coast also originated from the Gulf of Mexico after making landfall in the SUSA region or Florida Peninsula. It should be noted that in the SCHN SECHN, and SUSA regions, TC landfall angles to the coastline are more perpendicular, whereas the TC landfalls in the SEUS are more parallel to the coastline. As has been mentioned, the landfalling angle might impact the precipitation distribution of TCs during and after landfall.

*3.2. Overall TC rainfall asymmetries*

Fig. 2 displays the distribution of mean TC daily rainfall amount in SCHN, SECHN, SUSA, and SEUSA. TCs in the northwest Pacific basin (SCHN and SECHN; Fig. 2a–b) produce

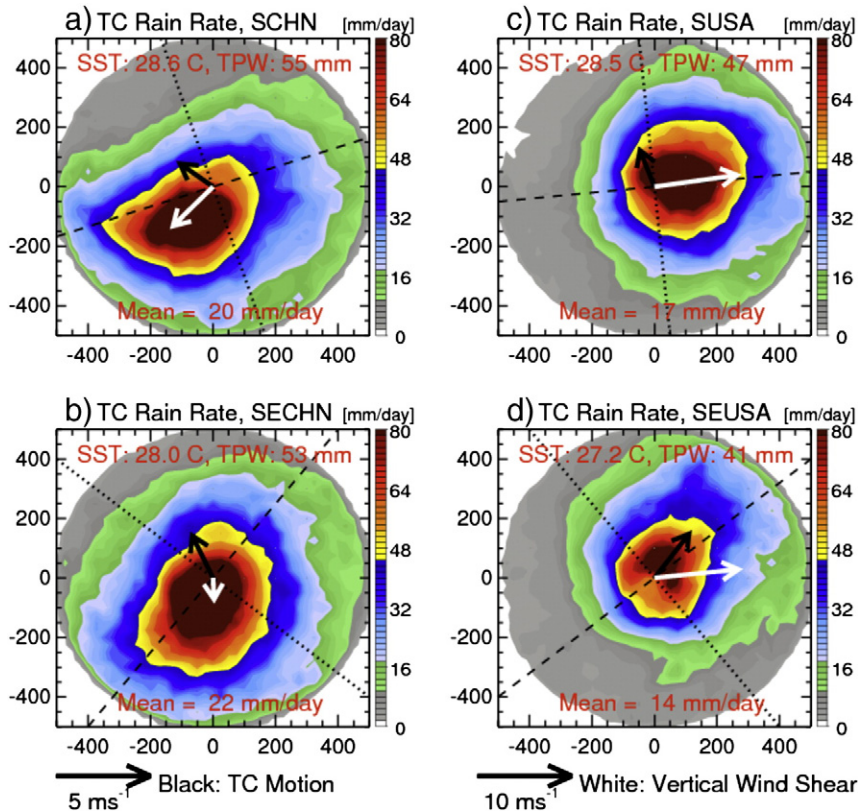


**Fig. 2.** Distribution of TC daily rainfall averaged in 1998–2011 over (a) SCHN, (b) SECHN, (c) SUSA, and (d) SEUSA. Black and white arrows represent TC motion and mean vertical wind shear (200–850 hPa), respectively. Dashed and dotted lines crossing the storm center are parallel and normal to the coast, respectively. Averaged SST and TPW are denoted by red text at the top, while mean rainfall rates at the bottom.

heavier precipitation and a larger rainfall area than those in the Atlantic basin (SUSA and SEUSA; Fig. 2c–d). This is mainly due to warmer waters (SST) and more TPW in the former region than the latter. All the regions show clear TC rainfall asymmetries. The most evident feature is that all regions have TC rainfall maxima located downshear (front quadrants) or downshear-left (front left quadrant) of vertical wind shear (Fig. 2 and Table 2). Although the rain rate magnitudes are greatest in the inner core, the magnitude of the asymmetry increases with distance (Table 2). Here, the asymmetry magnitude is simply defined as the ratio between precipitation rates in the favored quadrants and in the unfavored quadrants followed Cecil (2007). For example, the rainfall asymmetry magnitude under the high wind shear condition (e.g., SCHN, SUSA, and SEUSA; Fig. 2a,c, and d) is about 1.5 in the innermost 100 km, and increases to 2.0 and 3.0 at the radii of 200 and 300 km, respectively (Table 2). On the other hand, TC precipitation rates are slightly less asymmetric under the low shear environment (e.g., SECHN; Fig. 2b and Table 2). These general findings are consistent to previous case studies and satellite composites (Corbosiero and Molinari, 2002; Chan et al., 2004; Chen et al., 2006; Cecil, 2007). Numerical studies have shown certain mechanisms that make the downshear and downshear-left regions favored for upward motion and enhanced precipitation (Frank and Ritchie, 1999, 2001; Rogers et al., 2003; Ueno, 2007). These mechanisms involve downshear tilt of the TC vortex, secondary circulation (upward motion on the downtilt) due to vortex balance, vertical motion asymmetry produced by potential temperature anomalies, water vapor asymmetry due to vertical motion asymmetry, and cyclonic advection from the downshear region. In addition, the upward motion asymmetry is positively related to the magnitude of the vertical shear and intensity of the vortex (Ueno, 2007).

Certain studies demonstrated that storm motion effects on TC rainfall asymmetries (precipitation maxima ahead of the storm center) are quite substantial (Burpee and Black, 1989; Rodgers et al., 1994; Lonfat et al., 2004). However, in this study, three out of the four regions do not show TC rainfall maxima in the front quadrants of TC motion (black arrow; Fig. 2). Although SEUSA TCs displays front-maximum asymmetry (Fig. 2d), their front quadrants favored by storm motion actually overlap with the downshear-left quadrants favored by wind shear. Chen et al. (2006) and Ueno (2007) found that the downshear-left quadrant favored rainfall maxima are still evident even when storm motion is in the opposite direction or right of shear. Similarly, Corbosiero and Molinari (2002) showed that storm motion effects are secondary to that of wind shear in

**Table 2**

Direction (relative to wind shear) and magnitude of TC rainfall asymmetry as a function of distance from the TC center. Asymmetry direction is defined as the maximum precipitation quadrant (QUA) relative to wind shear, while asymmetry magnitude (MAG) is defined as the ratio of quadrant-averaged maximum and minimum precipitation. Quadrants include front-right (FR), front-left (FL), rear-right (RR), and rear-left (RL).

Region	0–100 km		100–200 km		200–300 km		300–400 km	
	QUA	MAG	QUA	MAG	QUA	MAG	QUA	MAG
SCHN	FL	1.94	FL	2.79	FL	3.00	FL	3.01
SECHN	FR	1.39	FR	1.88	FR	2.11	FR	2.59
SUSA	FL	1.64	FL	2.11	FL	3.13	FL	4.68
SEUSA	FL	1.46	FL	1.82	FL	3.51	FL	5.53

determining the asymmetric distribution of lightning flashes. The explanation is that storm motion-produced vertical motion asymmetries at the top of the boundary layer do not initiate deep convection if wind shear-induced circulations oppose them. In practice, storm motion itself should have an internal relationship with vertical wind shear. Ueno (2007) reported that TC motion in the western North Pacific tends to favor the right of the wind shear in the low-latitudes, whereas it favors the left of the wind shear in mid-latitudes.

### 3.3. TC rainfall asymmetry as a function of distance from the coast

Fig. 3 shows the TC rainfall distribution (in percentage of mean rainfall) as a function of distance of TCs from coast (Off-shore, Pre-land, Aft-land). In general, TCs prior to, during, and after landfall all display similar rainfall distribution. That is, most TCs have maximum rainfall located in the downshear (or downshear-left) quadrants. In other words, wind shear effects (see discussions in Section 3.2) dominate the rainfall distribution for the whole life cycle of landfalling TCs. Over the open oceans (Fig. 3a–d), TCs have far more rainfall in the downshear side (Fig. 3a–c), except for TCs in SEUSA (Fig. 3d). In SECHN (Fig. 3b), while the shear magnitude is relatively weak ( $<5 \text{ m s}^{-1}$ ), TC rainfall still favors the downshear quadrants. In contrast, TCs before landfalling in SEUSA are less asymmetric (asymmetries mainly in the most outer and light rain region), though the shear magnitude is substantial ( $7\text{--}10 \text{ m s}^{-1}$ ). It should be noted that SEUSA has relatively cool SST and small TPW and therefore limited rainfall area.

As TCs translate from the open ocean (Off-shore, Fig. 3a–d), approach the coast (Pre-land, Fig. 3e–h), and finally make landfall (Aft-land, Fig. 3i–l), the rainfall distribution experiences some noticeable changes. In SCHN and SECHN, TC rainfall percentage on the right side (relative to the coast) of the TC increases gradually in the outer rainband region (10–20%). The TC rainfall percentage in coastal regions to the right of TC center increases by more than 30% after the TC makes landfall. This indicates that the surface frictional convergence between the land and ocean plays some role in the rainfall enhancement in landfalling TCs (Powell, 1982; Blackwell, 2000; Chan et al., 2004). In the SUSA region, TC rainfall experiences a negligible rainfall (percentage) enhancement on the right side during the course of approaching the coast and making landfall. This can be explained by the fact that the right side of the TC motion in SUSA happens to be the downshear area where wind shear effect dominates the precipitation enhancement. In contrast, SEUSA TCs have an evident increase of rainfall percentage on the front-left quadrant of storm motion (but still right side relative to the coast) when TCs are close to landfall. The explanation is that TCs close to landfall in SEUSA recurve northward and graze the coast or make landfall on the left quadrants where friction gradient between the land and sea is present (Fig. 1b). In addition, the interaction between TCs and midlatitude systems also lead to precipitation maxima on the left of the track (Atallah et al., 2007). In many TCs that make landfall on the east coast of the US (especially north of North Carolina), the heaviest rains are found to the left (Atallah et al., 2007). Hurricane Sandy (2012) is such an example.

In mountainous coasts, topography could be a major factor that enhances TC rainfall due to the uplifting of TC

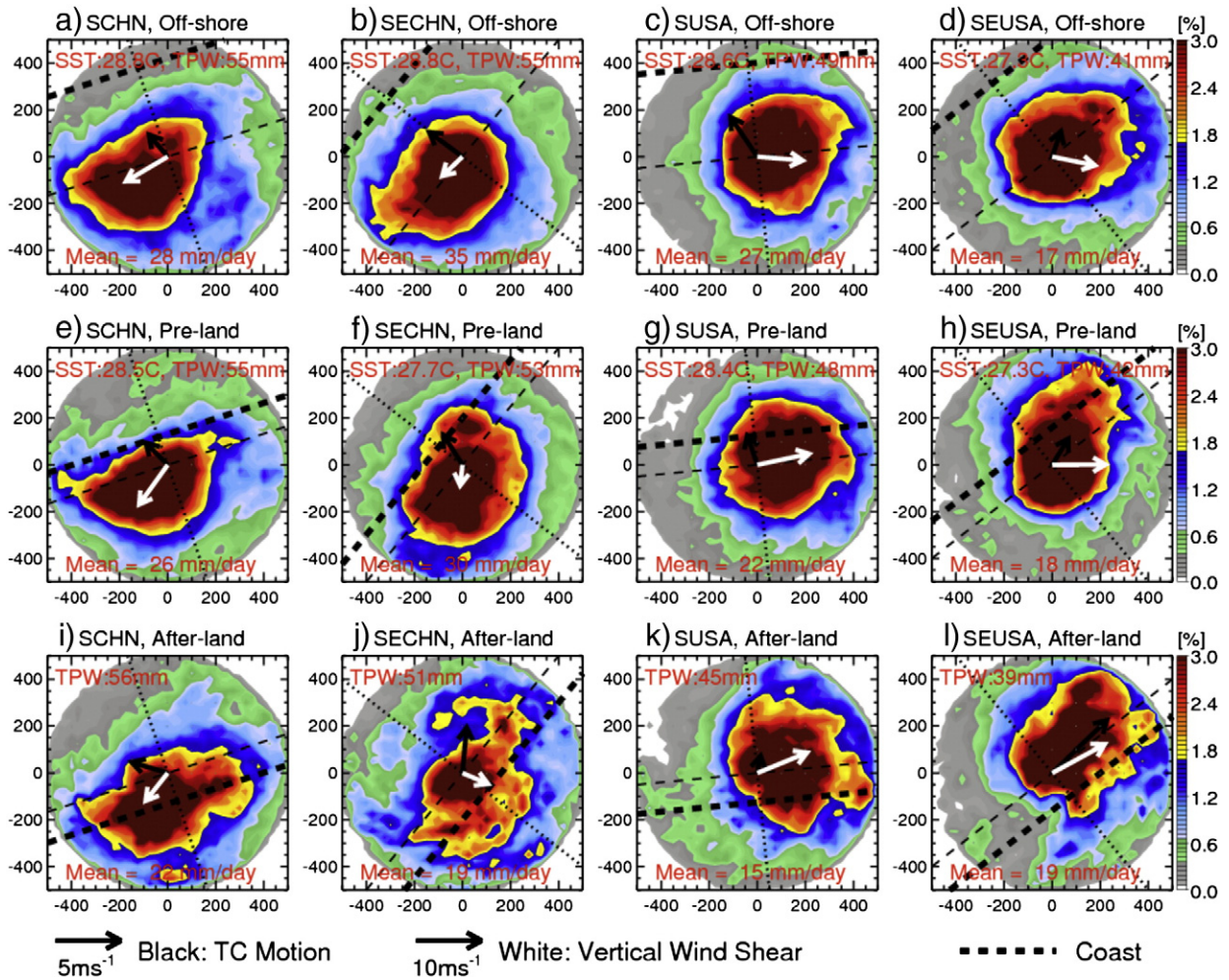


**Fig. 3.** Rainfall (in percentage of mean rainfall) distribution within 500 km radius of TCs at different stages of landfalling: (a)–(d): far away from coast (Off-shore), (e)–(h): prior to landfall (Pre-land), and (i)–(l): after-landfall (Aft-land). Thick dashed line is the approximate location of the coast.

flows when impinging on mountains (Chien and Kuo, 2011; Liou et al., 2012). In this study, TC rainfall enhancement by relatively low mountains (400–600 m) in SCHN and SECHN coasts is not evident when TCs made landfall and penetrated these mountains. Based on radar observations, Chan et al. (2004) pointed out that although bursts of convective cells can be seen in the vicinity of some isolated elevated locations in south China, the contribution of these terrains to the convective asymmetries (which are of the order of 100 km) were relatively small. Even though there is no signature of precipitation enhancement over the windward slopes in SCHN and SECHN, the topography might influence the TC rainfall through modifying the vertical wind shear. For example, low-level winds would be reduced when prevailing winds (e.g., westerlies) are approaching mountains over SCHN. This helps to enhance the northeasterly wind shear over this region, as the low-level southwesterly winds decrease. However, steep mountains in Taiwan (inside SECHN region) could cause major rainfall asymmetries. Pre-landfall TCs in SECHN (Fig. 3f and j) show clear rainfall maxima on the southern (also downshear) quadrants. These rainfall maxima

might not be caused by the wind shear effect, as the shear is very weak ( $2\text{--}3\text{ m s}^{-1}$ ). Instead, they are more likely caused by orographic lifting through TC flows impinging on steep mountains in central Taiwan, as most TCs in SECHN track near or over Taiwan. In many cases (40–50%), TCs cross Taiwan from the east and track down northwestward leading westerly flows in the southwest quadrant to impinge on the west side of central Taiwan mountains.

In this study, SST and TPW factors show a great influence on the extent and intensity of TC rainfall (Fig. 2), and slight impact on the TC rainfall asymmetry amplitude. In the warmer SST and larger TPW environment, wind shear effect on rainfall asymmetry tends to be more pronounced. For example, offshore TCs in SCHN, SECHN, and SUSA regions display a much greater magnitude of rainfall asymmetry, even under similar or smaller wind shear, than SEUSA where condition is cool and dry (Fig. 3a–d). Further study is needed to examine whether the dramatic rainfall asymmetry under weak shear environment is due to asymmetric distribution of SST and/or moisture field within the TC. On the other hand,

the interaction of TC outer circulation with the southwesterly flows might partially contribute to the rainfall maxima in the southern quadrants of TCs in western North Pacific. For example, Lee et al. (2012) reported that 22% typhoons in the western North Pacific are observed with long-lasting intense mesoscale convective systems (mainly in the southwest quadrant) due to the convergence between TC circulation and southwesterly low-level jets. Furthermore, this monsoon-TC interaction is a key factor in producing unexpected heavy precipitation by TC (e.g., Typhoon Marakot brought 1000–3000 mm to southern Taiwan in 4 days) (Chien and Kuo, 2011).

3.4. TC rainfall asymmetry as a function of TC intensity

This section analyzes TC rainfall distribution as a function of TC intensity (Fig. 4). TCs are limited to prior-to landfall (100–600 km from the coast), as most TCs degrade to tropical storms after landfall. In general, rainfall intensity increases as TC intensity increases due to the stronger circulation and dynamics in more intense TCs. However, the magnitude of TC rainfall

asymmetry decreases with increasing TC intensity. For example, CAT35 TCs have nearly symmetric rainfall distributions, and tropical storms show the most pronounced rainfall maxima in the downshear direction (Fig. 4a and b), while CAT12 TCs have a modest asymmetry. These results are consistent with previous studies based on satellite composites of TCs over global oceans (Chen et al., 2006; Cecil, 2007; Wingo and Cecil, 2010). The differences between asymmetry amplitude among the various intensity groups might be mainly due to the different primary circulation strength of the TC vortex. Tropical storms have a weaker and less organized (or less axisymmetric) circulation than CAT12 and CAT35 storms (Marks and Houze, 1987; Croxford and Barnes, 2002). In this case, the wind shear-induced asymmetric vertical motion is more substantial compared with the mean TC circulation. As a result, the deep convective activities on the downshear are more evident when they are initiated and enhanced by the asymmetric vertical motion. As the storm intensity increases, the primary circulation becomes stronger and more symmetric, and deep convection should be more symmetrically distributed around storm center.

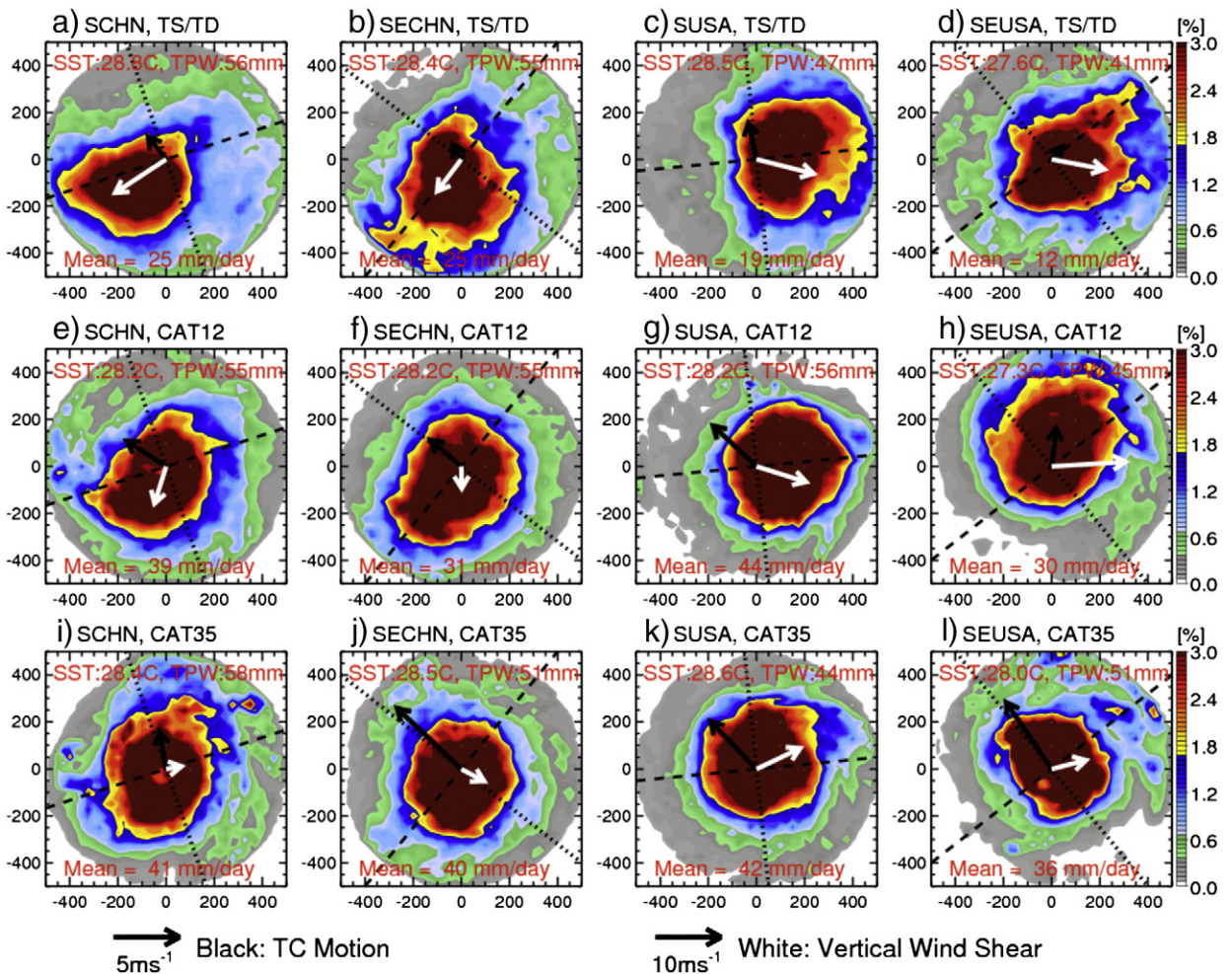


Fig. 4. Rainfall (in percentage of mean rainfall) distribution within 500 km radius of TCs prior to landfall (100–600 km from coast) in specific regions categorized by storm intensities (a)–(d): tropical storm or depression (TS/TD), (e)–(h): category one to two (CAT12), and (i)–(l): category three to five (CAT35).

Of course, the relationship between vertical wind shear magnitude and TC intensity should also be considered. Strong TCs are usually located in a low shear environment because they wouldn't have been able to intensify into a strong hurricane under high shear conditions. For example, CAT35 TCs in this study are under the weakest wind shear environment, especially for SCHN and SECHN where CAT35 TCs are under the shear of less than  $3 \text{ m s}^{-1}$  (Fig. 4i–j). There is no doubt that the shear effect is negligible under this situation. However, major hurricanes (CAT35) in SUSA experience substantial vertical wind shear ( $7\text{--}8 \text{ m s}^{-1}$ ) but not any significant rainfall asymmetry. In this case, the strong and symmetric TC circulation might be the key factor to symmetrically distribute rainfall. For TCs in TS/TD and CAT12 category, the wind shear factor predominantly determines the maximum rainfall location.

#### 4. Conclusions

This study examines landfalling TCs in South China and the Southeast US on the aspect of long-term (14-yr) averaged rainfall distribution as a function of TC distance from the coast, TC intensity, and other parameters such as SS and TPW. Statistics from this study are generally consistent with previous studies. This study further reveals that (1) the vertical wind shear (200–850 hPa) is a dominant factor in determining rainfall asymmetries (maxima on the downshear and downshear-left) even during landfalling or after-landfall periods, (2) the magnitude of the rainfall asymmetry decreases with increasing TC intensity even under substantial wind shear conditions, (3) effects of storm motion are not observed when vertical wind shear effects oppose them, (4) TCs close to landfall experience significant increase in the rainfall percentage toward the right quadrants relative to the coast, due to surface frictional gradient between land and sea (5) TC rainfall enhancement is only evident for TCs moving close to steep mountains (e.g., Taiwan), whereas low elevation mountains on the coast shows not any clear effects, and (6) the shear effect on rainfall asymmetry is more pronounced under the high SST and TPW environment than it is under the relatively cool SST and dry condition.

#### Acknowledgment

This research was supported by the NASA Precipitation Measurement Mission (PMM) Grant #NNX10AE28G. The authors would like to thank Joseph Zagrodnik (M.S. student at FIU) for his help on the English of the manuscript.

#### References

Atallah, E.H., Bosart, L.F., Ayyer, A.R., 2007. Precipitation distribution associated with landfalling tropical cyclones over the eastern United States. *Mon. Weather Rev.* 135, 2185–2206.

Blackwell, K.G., 2000. The evolution of Hurricane Danny 1997 at landfall: Doppler-observed eyewall replacement, vortex contraction/intensification, and low-level wind maxima. *Mon. Weather Rev.* 128, 4002–4016.

Burpee, R.W., Black, M.L., 1989. Temporal and spatial variations of rainfall near the centers of two tropical cyclones. *Mon. Weather Rev.* 117, 2204–2218.

Cecil, D.J., 2007. Satellite-derived rain rates in vertically sheared tropical cyclones. *Geophys. Res. Lett.* 34, L02811. <http://dx.doi.org/10.1029/2006GL027942>.

Chan, J.C.-L., Liu, K.-S., Ching, E., Lai, E.S.-T., 2004. Asymmetric distribution of convection associated with tropical cyclones making landfall along the South China coast. *Mon. Weather Rev.* 132, 2410–2420.

Chen, S.S., Knaff, J.A., Marks Jr., F.D., 2006. Effects of vertical wind shear and storm motion on tropical cyclone rainfall asymmetries deduced from TRMM. *Mon. Weather Rev.* 134, 3190–3208.

Chien, F.-C., Kuo, H.-C., 2011. On the extreme rainfall of Typhoon Morakot 2009. *J. Geophys. Res.* 116, D05104. <http://dx.doi.org/10.1029/2010JD015092>.

Corbosiero, K.L., Molinari, J., 2002. The effects of vertical wind shear on the distribution of convection in tropical cyclones. *Mon. Weather Rev.* 130, 2110–2123.

Croxford, M., Barnes, G.M., 2002. Inner core strength of Atlantic tropical cyclones. *Mon. Weather Rev.* 130, 127–139.

Dee, D.P., Uppala, S., 2009. Variational bias correction of satellite radiance data in the ERA-Interim reanalysis. *Q. J. R. Meteorol. Soc.* 135, 1830–1841.

Frank, W.M., Ritchie, E.A., 1999. Effects of environmental flow upon tropical cyclone structure. *Mon. Weather Rev.* 127, 2044–2061.

Frank, W.M., Ritchie, E.A., 2001. Effects of vertical wind shear on the intensity and structure of numerically simulated hurricanes. *Mon. Weather Rev.* 129, 2249–2269.

Habib, E., Henschke, A., Adler, R.F., 2009. Evaluation of TMPA satellite-based research and real-time rainfall estimates during six tropical-related heavy rainfall events over Louisiana, USA. *Atmos. Res.* 94, 373–388.

Huffman, G.J., et al., 2007. The TRMM multi-satellite precipitation analysis TMPA: quasi-global, multiyear, combined sensor precipitation estimates at fine scales. *J. Hydrometeorol.* 8, 38–55.

Jiang, H., Zipser, E.J., 2010. Contribution of tropical cyclones to the global precipitation from 8 seasons of TRMM data: regional, seasonal, and interannual variations. *J. Clim.* 23, 1526–1543. <http://dx.doi.org/10.1175/2009JCLI3303.1>.

Jiang, H., Halverson, J.B., Simpson, J., 2008a. On the differences in storm rainfall from Hurricanes Isidore and Lili. Part I: satellite observations and rain potential. *Weather Forecast.* 23, 29–43.

Jiang, H., Halverson, J.B., Zipser, E.J., 2008b. Influence of environmental moisture on TRMM-derived tropical cyclone precipitation over land and ocean. *Geophys. Res. Lett.* 35, L17806. <http://dx.doi.org/10.1029/2008GL034658>.

Jiang, H., Liu, C., Zipser, E.J., 2011. A TRMM-based tropical cyclone cloud and precipitation feature database. *J. Appl. Meteorol. Climatol.* 50, 1255–1274.

Knapp, K.R., Kruk, M.C., Levinson, D.H., Diamond, H.J., Neumann, C.J., 2010. The International Best Track Archive for Climate Stewardship (IBTrACS). *Bull. Am. Meteorol. Soc.* 91, 363–376. <http://dx.doi.org/10.1175/2009BAMS2755.1>.

Lee, C.-S., Chen, B.-F., Elsberry, R.L., 2012. Long-lasting convective systems in the outer region of tropical cyclones in the western North Pacific. *Geophys. Res. Lett.* 39, L21812. <http://dx.doi.org/10.1029/2012GL053685>.

Liou, Y.C., Wang, T.C.C., Tsai, Y.C., Tang, Y.S., Lin, P.L., Lee, Y.A., 2012. Structure of precipitating systems over Taiwan's complex terrain during Typhoon Morakot 2009 as revealed by weather radar and rain gauge observations. *J. Hydrol.* 506, 14–25.

Liu, K.S., Chan, J.C.L., Cheng, W.C., Tai, S.L., Wong, P.W., 2007. Distribution of convection associated with tropical cyclones making landfall along the South China coast. *Meteorol. Atmos. Phys.* 97, 57–68.

Lonfat, M., Marks Jr., F.D., Chen, S.S., 2004. Precipitation distribution in tropical cyclones using the Tropical Rainfall Measuring Mission (TRMM) microwave imager: a global perspective. *Mon. Weather Rev.* 132, 1645–1660.

Marks, F.D., Houze Jr., R.A., 1987. Inner core structure of Hurricane Alicia from airborne Doppler radar observations. *J. Atmos. Sci.* 44, 1296–1317.

Marks, F.D., Shay, L.K., 1998. Landfalling tropical cyclones: forecast problems and associated research opportunities. *Bull. Am. Meteorol. Soc.* 79, 305–323.

Matyas, C.J., 2010. Associations between the size of hurricane rain fields at landfall and their surrounding environments. *Meteorol. Atmos. Phys.* 106, 135–148.

Parrish, J.R., Burpee, R.W., Marks Jr., F.D., Grebe, R., 1982. Rain patterns observed by digitized radar during the landfall of Hurricane Frederic 1979. *Mon. Weather Rev.* 110, 1933–1944.

Powell, M.D., 1982. The transition of the Hurricane Frederic boundary-layer wind field from the open Gulf of Mexico to landfall. *Mon. Weather Rev.* 110, 1912–1932.

Prat, O.P., Nelson, B.R., 2014. Characteristics of annual, seasonal, and diurnal precipitation in the Southeastern United States derived from long-term remotely sensed data. *Atmos. Res.* <http://dx.doi.org/10.1016/j.atmosres.2013.07.022> (in press).

Rappaport, E.N., 2000. Loss of life in the United States associated with recent Atlantic tropical cyclones. *Bull. Am. Meteorol. Soc.* 81, 2065–2074.

Reynolds, R.W., Smith, T.M., Liu, C., Chelton, D.B., Casey, K.S., Schlax, M.G., 2007. Daily high-resolution blended analyses for sea surface temperature. *J. Clim.* 20, 5473–5496.

Rodgers, E.B., Chang, S., Pierce, H.F., 1994. A satellite observational and numerical study of precipitation characteristics in western North Atlantic tropical cyclones. *J. Appl. Meteorol.* 33, 129–139.

- Rogers, R., Chen, S.S., Tenerelli, J., Willoughby, H., 2003. A numerical study of the impact of vertical shear on the distribution of rainfall in Hurricane Bonnie 1998. *Mon. Weather Rev.* 131, 1577–1599.
- Shen, Y., Xiong, A., Wang, Y., Xie, P., 2010. Performance of high-resolution satellite precipitation products over China. *J. Geophys. Res.* 115, D02114. <http://dx.doi.org/10.1029/2009JD012097>.
- Shepherd, J.M., Grundstein, A., Mote, T.L., 2007. Quantifying the contribution of tropical cyclones to extreme rainfall along the coastal southeastern United States. *Geophys. Res. Lett.* 34, L23810. <http://dx.doi.org/10.1029/2007GL031694>.
- Tuleya, R.E., Kurihara, Y., 1978. A numerical simulation of the landfall of tropical cyclones. *J. Atmos. Sci.* 35, 242–257.
- Ueno, M., 2007. Observational analysis and numerical evaluation of the effects of vertical wind shear on the rainfall asymmetry in the typhoon inner-core region. *J. Meteorol. Soc. Jpn* 85, 115–136.
- Wingo, M.T., Cecil, D.J., 2010. Effects of vertical wind shear on tropical cyclone precipitation. *Mon. Weather Rev.* 138, 645–662.
- Zhao, T., Yatagai, A., 2013. Evaluation of TRMM 3B42 product using a new gauge-based analysis of daily precipitation over China. *Int. J. Climatol.* <http://dx.doi.org/10.1002/joc.3872>.